Spatial patterns of water diffusion along white matter tracts in temporal lobe epilepsy

Luis Concha, MD, PhD
Hosung Kim, PhD
Andrea Bernasconi, MD
Boris C. Bernhardt, PhD
Neda Bernasconi, MD, PhD

Correspondence & reprint requests to Dr. Bernasconi neda@bic.mni.mcgill.ca

ABSTRACT

Objectives: Diffusion tensor imaging (DTI) tractography has shown tract-specific pathology in temporal lobe epilepsy (TLE). This technique normally yields a single value per diffusion parameter per tract, potentially reducing the sensitivity for the detection of focal changes. Our goal was to spatially characterize diffusion abnormalities of fasciculi carrying temporal lobe connections.

Methods: We studied 30 patients with drug-resistant TLE and 21 healthy control subjects. Twenty-four patients underwent DTI toward the end of video-EEG telemetry, with an average of 50 ± 54 hours between the last seizure and DTI examination. After manual dissection of the uncinate and inferior longitudinal and arcuate bundle, they were spatially matched based on their distance to the temporal lobe, providing between-subject correspondence of tract segments. We evaluated point-wise differences in diffusion parameters along each tract at group and subject levels.

Results: Our approach localized increased mean diffusivity restricted to or more prominent within the ipsilateral temporal lobe. These abnormalities tapered off as tracts exited the temporal lobe. We observed that the shorter the interval between the last seizure and DTI, the higher the mean diffusivity (MD) of the ipsilateral tracts. Linear discriminant analysis of tract segments correctly lateralized 87% of patients.

Conclusions: The centrifugal pattern of white matter diffusion abnormalities probably reflects astrogliosis and microstructure derangement related to seizure activity in the vicinity of the focus. The negative correlation between the interval from last seizure and MD suggests a role for postictal vasogenic edema. The ability to assess tracts segmentally may contribute to a better understanding of the extent of white matter pathology in epilepsy and assist in the presurgical evaluation of patients with TLE, particularly those with unremarkable conventional imaging results. ***Neurology*® 2012;79:455–462**

GLOSSARY

DTI = diffusion tensor imaging; **FA** = fractional anisotropy; **FWHM** = full-width at half-maximum; **MD** = mean diffusivity; **TE** = echo time; **TLE** = temporal lobe epilepsy; **TR** = repetition time; **WM** = white matter.

Although hippocampal sclerosis is a hallmark of temporal lobe epilepsy (TLE) and its diagnosis is crucial for the lateralization of the seizure focus, MRI morphometry has shown bilateral widespread gray matter atrophy.[1-3] Conversely, white matter (WM) morphometry has shown atrophy[1,4,5] and increased T2 signal intensity,[6,7] more restricted to frontotemporal regions ipsilateral to the seizure focus.

Morphometry is a sensitive indicator of pathology. Its ability to convey information regarding tissue architecture is nevertheless limited. Alternatively, diffusion tensor imaging (DTI), a technique sensitive to the spatial displacement of water molecules,[8] allows making inferences about microstructural integrity of axons and myelin sheaths through the analysis of diffusivity perpendicular and parallel to the tracts.[9] By estimating the diffusion tensor, DTI tractography allows 3-dimensional depiction of WM tracts.[10] In TLE, tractography has been mainly used as a segmentation tool for

Supplemental data at www.neurology.org

Supplemental Data

From the Neuroimaging of Epilepsy Laboratory (C.L., H.K., A.B., N.B.), Montreal Neurological Institute and Hospital, Montreal; and Department of Neurology and Neurosurgery and McConnell Brain Imaging Center (A.B.), McGill University, Montreal, Canada.

Study funding: Supported by the Canadian Institutes of Health Research (CIHR MOP-57840 and CIHR MOP-93815). L.C was funded by the Canadian Institutes of Health Research and Savoy Foundation for Epilepsy.

Go to Neurology.org for full disclosures. Disclosures deemed relevant by the authors, if any, are provided at the end of this article.

Table Demographic and clinical data of patients

	Male	Age, y	Onset, y	Lateralization	Volumetry	Surgery	Outcome
1.5 T							
Control (n = 10)	6	31 ± 7 (21–42)					
TLE (n = 18)	9	30 ± 9 (16–49)	14 ± 5 (5–23)	11 LT 7 RT	15HA 3NV	14	12 (I) 2 (II)
3.0 T							
Control (n = 11)	5	30 ± 8 (20–48)	—	—	—	—	—
TLE (n = 12)	5	29 ± 8 (19–40)	14 ± 5 (5–25)	7 LT 5 RT	8HA 4NV	10	8 (I) 1 (II) 1 (III)

Abbreviations: HA = patients with hippocampal atrophy; NV = patients with normal hippocampal volume; LT = left temporal seizures as determined by video-EEG monitoring; RT = right temporal seizures.
[a] Age and onset of epilepsy are presented as mean ± SD (range). Outcome refers to Engel postsurgical classification.

whole-tract analyses, providing the mean value of diffusion parameters for the entire tract.[11] A global estimation of diffusion characteristics has limited sensitivity to detect subtle diffuse or focal changes. The goal of this study was to spatially characterize WM diffusion abnormalities along the trajectory of tracts related to the temporal lobe in drug-resistant TLE. We used subject-specific tractography bundle segmentation. After between-subject correspondence was obtained through an atlas-independent approach based on tract length,[12] we mapped groupwise differences between patients and control subjects onto the trajectories of the tracts. Furthermore, we assessed the reliability of pointwise analysis to lateralize the seizure focus compared with the whole-tract approach.

METHODS

Subjects. We studied 30 consecutive patients with drug-resistant TLE undergoing presurgical evaluation at the Montreal Neurological Hospital (16 female; mean age 30 ± 9 years; right-handed) and 21 healthy control subjects matched for age, sex, and handedness (10 female; mean age 30 ± 7 years). Demographic and clinical data were obtained through interviews with the patients and their relatives (table). Diagnosis and lateralization of the seizure focus into the left TLE and right TLE were determined by a comprehensive evaluation including detailed history, seizure semiology, video-EEG recordings, and neuroimaging. All patients had unilateral temporal lobe seizures. None of the patients had a mass lesion (cortical, tumor, or vascular malformations) or traumatic brain injury.

Twenty-four patients (80%) were studied during their hospitalization that lasted on average 10 ± 3 days (range 7–20 days). Fifteen of them (63%) underwent the MRI examination on the last day of video-EEG telemetry and 9 toward the end of this investigation, when their antiepileptic medication was either reduced or suspended. The time interval between the last seizure and the MRI scan was on average 50 ± 54 hours (range 5 minutes–8 days). The 6 remaining patients were examined as outpatients. Five of them had a seizure 1 week before the examination and one 10 minutes before.

Twenty-four patients (80%) were operated on, 4 were awaiting surgery, and 2 refused surgery. We determined outcome according to the Engel classification scheme,[13] at a mean follow-up of 38 ± 20 months. Twenty patients (83%) had an outcome of class I, 3 (12.5%) of class II, and 1 of class III. Qualitative pathologic examination of the resected tissue revealed hippocampal sclerosis in all patients.

Standard protocol approvals, registration, and patient consents. The Ethics Committee of the Montreal Neurological Institute and Hospital approved the study, and written informed consent was obtained from all participants.

MRI acquisition and image processing. MR images were acquired on a 1.5-T Siemens Sonata scanner in the first 18 patients with TLE (9 female; mean age 30 ± 9 years) and in 10 healthy control subjects (4 female; mean age 31 ± 7 years) using an 8-channel phased-array head coil. After the upgrade of our MRI hardware, the subsequent 12 patients (7 female; mean age 29 ± 8 years) and 11 healthy control subjects (6 female; mean age 30 ± 8 years) were examined on a 3.0-T Siemens Trio Tim scanner using a 32-channel phased-array head coil. The DTI protocol consisted of a twice-refocused echo-planar imaging sequence. On the 1.5-T scanner, 54 axial slices were acquired with a voxel resolution of 2.5 × 2.5 × 2.5 mm^3, repetition time (TR) = 7.5 seconds, and echo time (TE) = 94 msec, with diffusion-sensitized images in 30 directions with b = 1,000 s/mm^2, along with 5 non–diffusion-weighted volumes (number of excitations = 2). On the 3.0-T scanner, 63 axial slices were acquired with a voxel resolution 2 × 2 × 2 mm^3, TR = 8.4 seconds, and TE = 90 msec, with diffusion-sensitized images in 64 directions with b = 1,000 s/mm^2 and 1 non–diffusion-weighted volume.

T1-weighted images were acquired on each scanner using a 3-dimensional magnetization-prepared rapid-acquisition gradient echo, providing isotropic voxels of 1 × 1 × 1 mm. Images underwent automated correction for intensity nonuniformity and intensity standardization[14] and were linearly registered into a standardized stereotaxic space.[15] The hippocampus was segmented manually according to our previously described protocol.[16] Based on 2 SD below mean absolute volume or interhemispheric asymmetry in healthy control subjects, 23 patients had unilateral atrophy ipsilateral to the seizure focus and 7 had normal hippocampal volumes.

DTI tractography. Each volume in the DTI dataset was linearly registered to the first non–diffusion-weighted volume to

Figure 1 Distance estimation along the trajectory of the tract

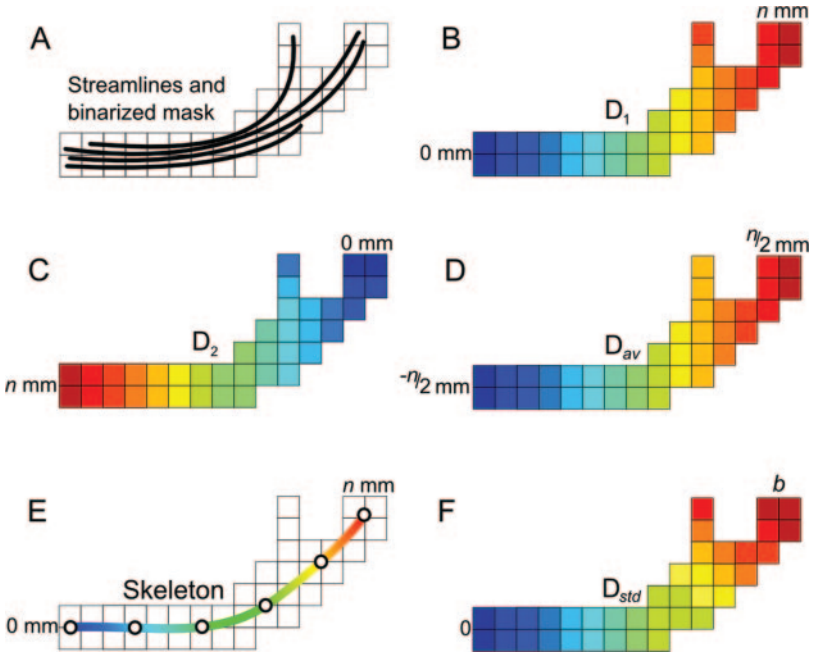

(A) Diffusion tensor imaging–derived tracts (streamlines) are used to create a binary mask of the tract. (B, C) For each voxel, its distance to both the start and end of this mask is computed using a distance transformation. (D, E) A tract skeleton is obtained from the average of these 2 values, which is then interpolated using a B-spline (E). (F) The tract skeleton is used to parameterize the distance into *b* number of bins ($b = 50$ in our case) without bias from tract branches.

Figure 2 Distance profiling

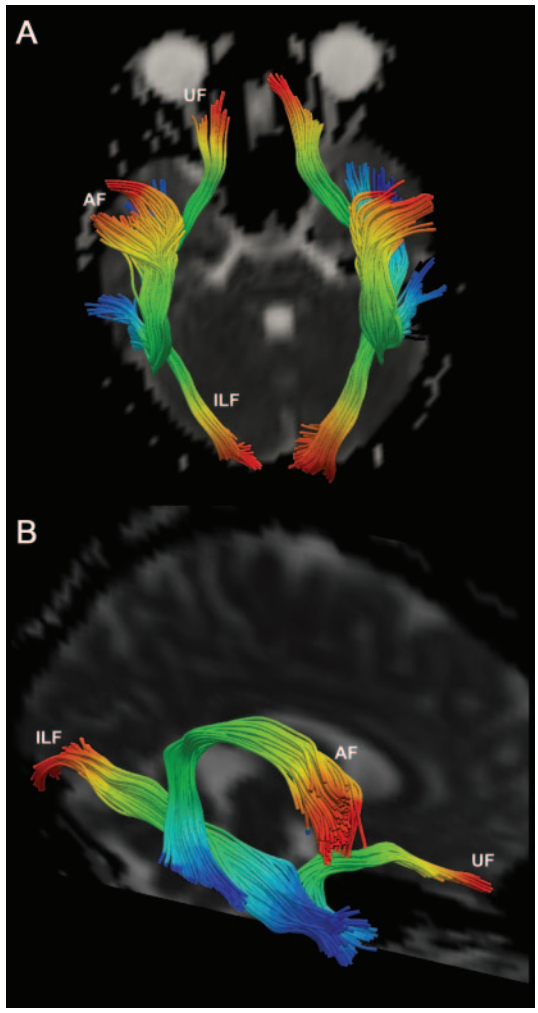

Profiles of the uncinate (UF), inferior longitudinal (ILF), and arcuate fasciculi (AF) overlaid on a non–diffusion-weighted volume shown in axial (A) and oblique (B) views. Each tract is divided into 50 color-coded bins, from start (blue) to end (red).

minimize within-scan bulk motion. Tensor calculation, diagonalization, and tractography were performed using the software package MedINRIA 1.8.[17] Streamline tractography was performed in native space, initiated in all voxels with a fractional anisotropy (FA) value > 0.2.

We selected the uncinate, inferior longitudinal, and arcuate fasciculi, fiber tracts that carry connections of the temporal lobe. These bundles were individually dissected by manually placing 2 large tract-selection regions on coronal slices using guidelines from WM atlases.[18,19] In short, we first identified the lobar poles (temporal, frontal, and occipital) and then moved progressively along slices until the WM became visible, where tract-selection regions were drawn. For the uncinate and inferior longitudinal fasciculi, the first tract-selection region was placed at the temporal pole. The second region was placed at the frontal pole (uncinate) and occipital pole (inferior longitudinal fasciculus). The first tract-selection region for the arcuate fasciculus was placed in the superior temporal gyrus and the second in the frontal lobe WM. Both regions were drawn on a coronal slice at the level of the posterior edge of the internal capsules. The start and end points of all tracts were carefully assessed to be in the same anatomic locations for all subjects and only the portions of the tracts between the 2 selection regions were retained for analysis.

Mapping water diffusion parameters along the trajectory of the tracts. We have recently developed a method to analyze diffusion along WM tracts.[12] The steps are summarized in figure 1. Each tract is converted into a binarized volume. With use of the Chamfer algorithm, distances from each voxel in the tract's mask to both its start and end points are computed and averaged. The set of mean positions is then interpolated using a cubic B-spline curve. This curve represents the skeleton of the tract, thus allowing a smooth representation that is impervious to branches. The distance from the start point of the B-spline skeleton is then estimated. To standardize distances across subjects, the distance profile of the tract skeleton was partitioned into *b* portions (or bins) as $D_{std}(s) = b\,(D(s)/D_{end})$, where $D(s)$ is the distance value at any given point s on the skeleton and D_{end} is the maximum distance at the end point. Finally, the distance of each voxel x in the binary tract mask corresponds to the distance in the skeleton by $D(x) = \arg\min_d \|x - s(D_{std} = d)\|$, where $s(D_{std} = d)$ is a point on the skeleton with a standardized distance d. Note that the skeleton itself is not analyzed but rather all the voxels in the tract's mask after the estimation of their distance to the start point of the tract. The number of bins (b) was set to 50 to include at least 4 voxels per bin per tract. The starting positions for all fasciculi were in the temporal lobe (figure 2).

FA, mean (MD), parallel (D_{par}), and perpendicular diffusivities (D_{perp}) were calculated from the eigenvalues of the diffusion tensor (namely λ_1, λ_2, and λ_3), with $D_{par} = \lambda_1$ and $D_{perp} = (\lambda_2 + \lambda_3)/2$. These 4 diffusion parameters were averaged across all voxels at each bin and plotted against their respective distance

bins. We then smoothed the diffusion parameters along the normalized length of the tracts using a Gaussian kernel with a full-width at half-maximum (FWHM) of 2.5 bins. We calculated the effective smoothness ($FWHM_{eff}$) that takes into consideration not only the smoothness introduced by the blurring operation but also the intrinsic smoothness of the data, and its estimation is necessary for statistical analysis using random field theory.[20]

Statistical analysis. We conducted our analysis using the SurfStat toolbox for Matlab (R2007a). For each DTI dataset (1.5 and 3.0 T), patients were analyzed relative to the epileptogenic lobe (i.e., ipsilateral and contralateral to the seizure focus). To this purpose, we normalized the diffusion parameters at each bin using a *z* transformation with respect to the distribution of the corresponding hemisphere of controls (i.e., each patient's right/left parameter was expressed as a *z* score with respect to the right/left values of control subjects for each dataset).

Group analysis. We evaluated bin-wise differences in diffusion parameters along each tract using one-tailed Student *t* tests. Analyses were first performed separately for 1.5- and 3.0-T data. Because group comparisons showed similar results (figure e-1 on the *Neurology*® Web site at www.neurology.org), we report findings for the combined datasets. In a separate analysis, we assessed groupwise differences using the conventional whole-tract approach (averaging diffusion parameters of the entire tract, thus disregarding spatial information).

Clinical analysis. We evaluated the relation of hippocampal volume and time interval between last seizure and imaging to bin-wise DTI parameters using linear models. In clusters of groupwise diffusion anomalies, we assessed the effects of postsurgical outcome.

Seizure focus lateralization. To assess the ability of DTI parameters to lateralize the seizure focus in patients with TLE, we performed a linear discriminant analysis. We cross-validated the model using a leave-one-out procedure by which a patient is classified (as left TLE or right TLE) using the data of all patients other than that patient. This allows an unbiased assessment of lateralization performance for previously unseen patients with TLE. The discriminant analysis was performed on the bin-wise as well as on the whole-tract data.

Correction for multiple comparisons. We corrected significances for bin-wise analyses using random field theory on a cluster level, thereby controlling for the chance of ever reporting a false-positive finding to be less than 0.05. The number of contiguous bins showing a statistically significant difference at $p < 0.05$ was divided by the $FWHM_{eff}$ of the smoothing kernel to obtain the cluster's size in resels (a measure of the number of resolution elements in the statistical map). This can be thought of as similar to the number of independent observations.[20] Clusters were considered significant if their size in resels was larger than the threshold obtained from random field theory at $\alpha = 0.05$.

RESULTS

Spatial analysis along tracts. Results are shown in figures 3 and 4. Ipsilateral to the seizure focus, the uncinate and inferior longitudinal fasciculi showed abnormally increased MD throughout their length (a reflection of simultaneous increase in D_{par} and D_{perp}), although these abnormalities were always more severe in temporal segments. Conversely, increased MD was restricted to the temporal portion of the arcuate fasciculus. We found reduced FA in the ipsilateral temporal portion of the uncinate fasciculus. Contralateral increased MD was less marked and mainly present in the temporal portion of the inferior longitudinal and the uncinate fasciculi, with the latter displaying additional anomalies located in its frontal segment. Repeating the bin-wise group analysis in the subset of patients with normal hippocampal volumetry revealed the same pattern of abnormalities in the 3 tracts studied (i.e., localized diffusion alterations restricted to or more prominent within the ipsilateral temporal lobe). Bin-wise group differences were robust to changes of FWHM used for filtering the data.

Figure e-2 shows the bin-wise percentage of patients with abnormal diffusion parameters plotted against length of tracts. Up to 40% of patients exhibited ipsilateral MD values 2 SD above the mean of control subjects in the temporal portions of the 3 fasciculi. Decreased FA was present in approximately 20% of patients and was distributed more homogeneously along the tracts.

Conventional whole-tract analysis. For the whole-tract analysis, the most notable abnormalities were seen for MD, D_{par}, and D_{perp} of the 3 tracts studied, ipsilateral to seizure focus (figure e-3).

Clinical analysis. We found a negative correlation between time from last seizure and MD in the ipsilateral distal portion of the all 3 tracts. Conversely, we did not find any correlation between hippocampal volume and bin-wise diffusion along WM tracts. With respect to postsurgical outcome, comparing mean changes in clusters of diffusion anomalies between groups revealed trends for increased MD in the ipsilateral arcuate ($p = 0.01$ uncorrected) and inferior longitudinal fasciculus ($p = 0.04$ uncorrected) in patients who became seizure-free (Engel class I) compared with those with residual seizures after surgery (Engel classes II–IV).

Seizure focus lateralization. To lateralize the seizure focus, we used diffusion parameters of the inferior longitudinal fasciculus, because it yielded the strongest groupwise differences. We obtained in each patient MD values within clusters of groupwise difference (figure 3) and fed them to a linear discriminant classifier. This allowed correct lateralization in 87% of patients, including 91% (21 of 23) with hippocampal atrophy and 71% (5 of 7) with normal volume. Conversely, MD data from the whole-tract analyses yielded correct lateralization only in 70% of patients.

DISCUSSION

We performed a quantitative analysis of the spatial distribution of diffusion parameters along the uncinate, arcuate, and inferior longitudinal

Figure 3 Group comparisons

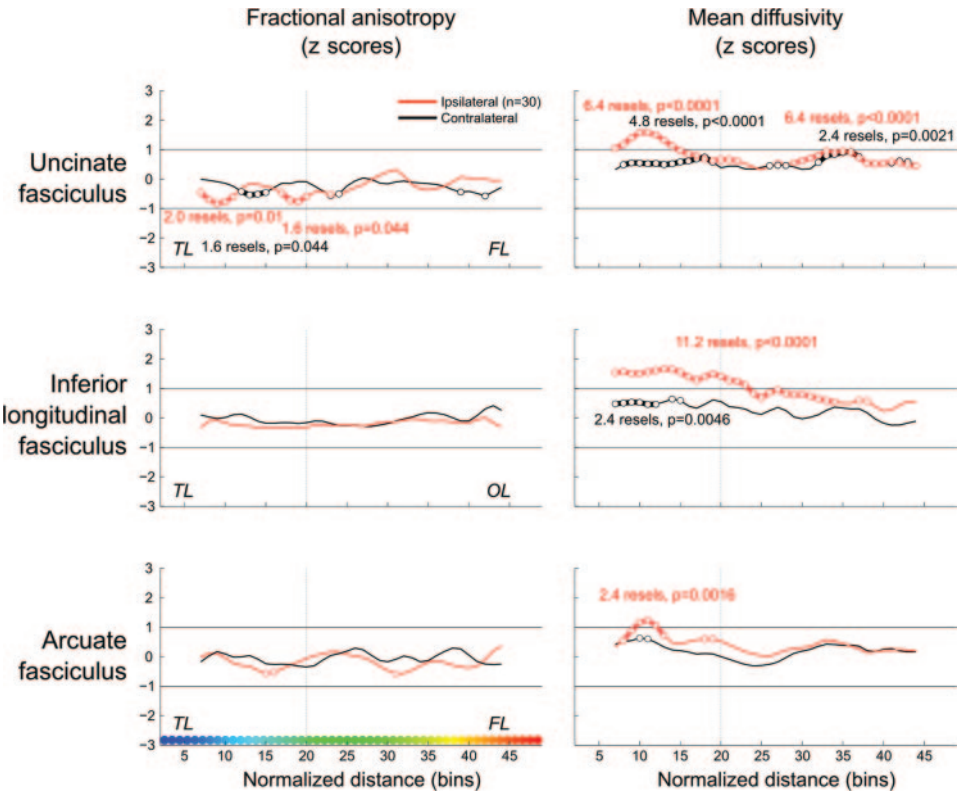

z scores of mean diffusivity and fractional anisotropy plotted along the normalized length of the tracts (color-coded on the x-axis, left lower panel). Bin-wise average values of patients with temporal lobe epilepsy are compared with those obtained from the corresponding hemisphere (i.e., left or right) of healthy control subjects (0 on the y-axis represents the mean in healthy control subjects). Clusters of significant differences after random field theory correction are shown as circles. The vertical dashed lines on each graph separate the temporal (TL) from the frontal (FL) and occipital lobe (OL) portions of the tracts.

fasciculi. We used random field theory as a robust statistical framework for correction of multiple comparisons. We found localized diffusion alterations restricted to or more prominent within the ipsilateral temporal lobe. The centrifugal pattern of WM microstructural pathology tapering off as tracts exit the temporal lobe probably reflects astrogliosis related to chronic seizure activity in the vicinity of the focus, rather than being due to hippocampal damage. Indeed, repeating the bin-wise group analysis in the subset of patients with normal hippocampal volumetry revealed the same pattern of abnormalities. In addition, we did not find a correlation between hippocampal volume and diffusion anomalies along WM tracts. Hippocampal neuronal loss has been linked to progressively reduced volume of the fornix, its major output.[21] Nonetheless, because the 3 fasciculi we studied do not carry direct hippocampal efferents, it would be unexpected to find a correlation between their microstructural integrity and hippocampal volume. An alternate explanation for the centrifugal pattern is that axonal and myelin pathology may be consistent throughout the length of the tract, but the proportion of altered axons may decrease as intact axons distant from the epileptogenic tissue join the fascicle.

Whole-tract approaches may miss focal abnormalities, particularly when they occur in a small fraction of the tract. Indeed, the abnormally high diffusivity seen in the temporal portion of the arcuate fasciculus was not evident in the whole-tract analysis. The conventional approach also missed contralateral anomalies and yielded lower lateralization performance than our segmental analysis. We found trends for increased MD ipsilateral to the seizure focus in patients who became seizure-free compared with those who had residual seizures after surgery. Although these results have to be taken cautiously because of unbalanced outcome groups, they add to the body of evidence showing that structural damage, ipsilateral to the seizure focus, has significant prognostic value in epilepsy surgery.[22] Taken together, our results suggest that characterization of diffusion profiles of WM tracts may be of clinical value in assisting in the presurgical evaluation of patients with TLE, both in term of lateralization, particularly in those

Figure 4 Group comparisons

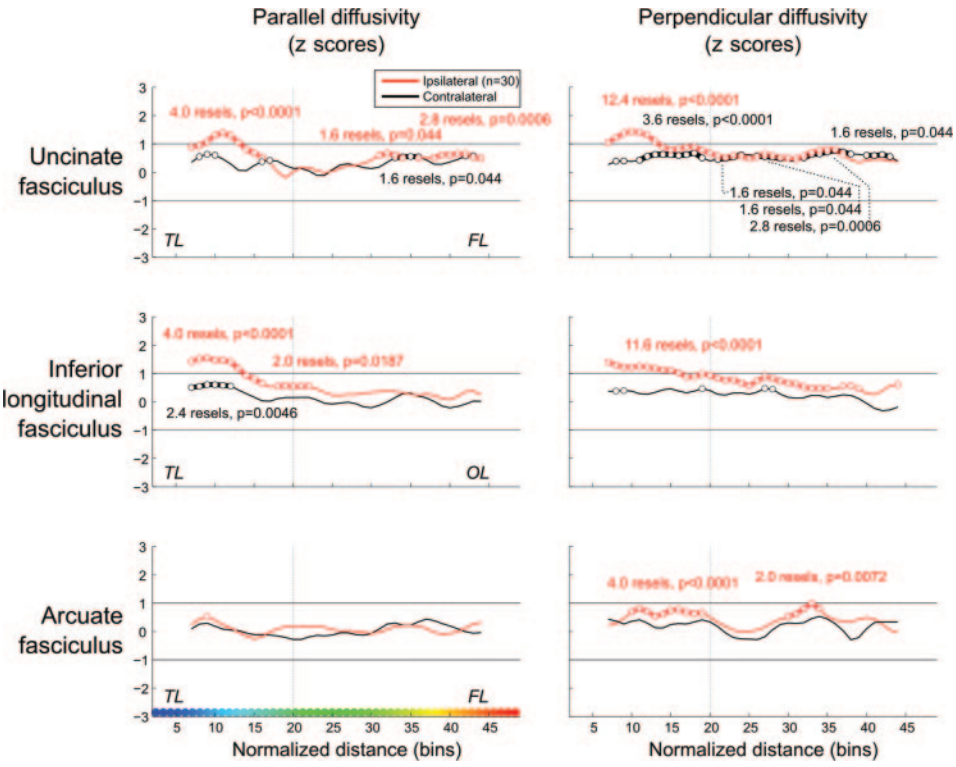

z scores of parallel and perpendicular diffusivities along the normalized length of tracts. Bin-wise average values of patients with temporal lobe epilepsy are compared with those obtained from the corresponding hemisphere (i.e., left or right) of healthy control subjects (0 on the y-axis represents the mean in healthy control subjects). For details, see the legend to figure 3.

with unremarkable conventional imaging, and outcome prediction.

Previous reports have demonstrated that alterations in MD vary with respect to the dynamics of seizure activity.[23] In the hyperacute phase after prolonged seizures or status epilepticus, there is a decrease in MD due to intracellular cytotoxic edema. In the subacute peri-ictal phase, which may last up to 5 days,[24] an increase in MD occurs in relation to vasogenic edema. The chronic phase is associated with neuronal loss and gliosis, leading to further MD increase as a consequence of the expansion of the interstitial water content. Gliotic changes of temporal lobe WM are indeed common in TLE.[25,26] The majority of patients included in this study had undergone prolonged monitoring with reduced or no medication, leading to increased seizure frequency in the days before imaging. We found that the shorter the interval between the last seizure and the DTI was, the higher the MD of ipsilateral tracts. These results are in line with reports of elevated MD in the subacute postictal state.[27,28] Notably, group comparisons revealed increased MD mainly in the temporal portion of the tracts, whereas effects of time form last seizure were observed in the distal, extratemporal segments. Hence, analysis of tract segments allowed disentangling potential pathophysiologic mechanisms, with the temporal portion showing signs of static microstructural damage due to chronic seizure activity, whereas changes in the distal portion seem to be modulated by postictal edema.

Mechanisms governing microstructural WM abnormalities within a given fascicle may differ with respect to its relation to the hippocampus. Previous DTI studies have shown that WM bundles directly related to the temporal neocortex present with more prominent abnormalities in the epileptogenic hemisphere,[29-31] whereas limbic pathways such as the fornix and cingulum are affected bilaterally.[29,30,32] Regardless of laterality, it is notable that our FA findings were relatively minimal and mainly seen along the ipsilateral temporal portion of the uncinate bundle. Because of the divergence in time interval between seizure activity and DTI acquisition, a direct comparison between studies is difficult. In our cohort, the relative lack of FA variations may be due to the short interval between the last seizure, along with the cumulative effect of increased seizure frequency during video-EEG telemetry, and the DTI examination. A reduction in FA is thought to reflect decreased axonal density and altered myelin membrane integrity.[33] Although water diffusion is perturbed

chronically, a transitory increase in diffusivity due to peri-ictal vasogenic edema may augment the likelihood of water molecules to encounter tissue barriers, thus maintaining anisotropy and masking chronic FA decreases.

AUTHOR CONTRIBUTIONS

L. Concha: drafting manuscript for content, including medical writing; study concept and design; statistical analysis and interpretation of data. A. Bernasconi: revising manuscript for content, including medical writing; interpretation of data; study supervision; obtaining funding. H. Kim: analysis and interpretation of data. B. C. Bernhardt: analysis and interpretation of data. N. Bernasconi: revising manuscript for content, including medical writing; study concept and design; interpretation of data; acquisition of data; study supervision; obtaining funding.

ACKNOWLEDGMENT

The authors thank Drs. K. Worsley and F. Carbonell for their advice on the statistical analysis.

DISCLOSURE

The authors report no disclosures relevant to the manuscript. **Go to Neurology.org for full disclosures.**

Received November 1, 2011. Accepted in final form March 19, 2012.

REFERENCES

1. Bernasconi N, Duchesne S, Janke A, Lerch J, Collins DL, Bernasconi A. Whole-brain voxel-based statistical analysis of gray matter and white matter in temporal lobe epilepsy. Neuroimage 2004;23:717–723.
2. Bonilha L, Rorden C, Halford JJ, et al. Asymmetrical extra-hippocampal grey matter loss related to hippocampal atrophy in patients with medial temporal lobe epilepsy. J Neurol Neurosurg Psychiatry 2007;78:286–294.
3. Bernhardt BC, Bernasconi N, Concha L, Bernasconi A. Cortical thickness analysis in temporal lobe epilepsy: reproducibility and relation to outcome. Neurology 2010; 74:1776–1784.
4. McMillan AB, Hermann BP, Johnson SC, Hansen RR, Seidenberg M, Meyerand ME. Voxel-based morphometry of unilateral temporal lobe epilepsy reveals abnormalities in cerebral white matter. Neuroimage 2004;23:167–174.
5. Seidenberg M, Kelly KG, Parrish J, et al. Ipsilateral and contralateral MRI volumetric abnormalities in chronic unilateral temporal lobe epilepsy and their clinical correlates. Epilepsia 2005;46:420–430.
6. Pell GS, Briellmann RS, Pardoe H, Abbott DF, Jackson GD. Composite voxel-based analysis of volume and T2 relaxometry in temporal lobe epilepsy. Neuroimage 2008; 39:1151–1161.
7. Townsend TN, Bernasconi N, Pike GB, Bernasconi A. Quantitative analysis of temporal lobe white matter T2 relaxation time in temporal lobe epilepsy. Neuroimage 2004;23:318–324.
8. Basser PJ, Mattiello J, Le Bihan D. MR diffusion tensor spectroscopy and imaging. Biophys J 1994;66:259–267.
9. Beaulieu C. The basis of anisotropic water diffusion in the nervous system: a technical review. NMR Biomed 2002; 15:435–455.
10. Mori S, van Zijl PC. Fiber tracking: principles and strategies: a technical review. NMR Biomed 2002;15:468–480.
11. Yogarajah M, Duncan JS. Diffusion-based magnetic resonance imaging and tractography in epilepsy. Epilepsia 2008;49:189–200.
12. Concha L, Kim H, Bernhardt B, Bernasconi N. A framework for the statistical analysis of focal water diffusion abnormalities along white matter tracts. Presented at MICCAI Workshop on "Diffusion Modelling"; September 24, 2009, London.
13. Engel J Jr, Van Ness PC, Rasmussen T, Ojemann LM. Outcome with respect to epileptic seizures. In: Engel J Jr, ed. Surgical Treatment of the Epilepsies, 2nd ed. New York: Raven Press; 1993:609−621.
14. Sled JG, Zijdenbos AP, Evans AC. A nonparametric method for automatic correction of intensity nonuniformity in MRI data. IEEE Trans Med Imaging 1998; 17:87–97.
15. Collins DL, Neelin P, Peters TM, Evans AC. Automatic 3D intersubject registration of MR volumetric data in standardized Talairach space. J Comput Assist Tomogr 1994;18:192–205.
16. Bernasconi N, Bernasconi A, Caramanos Z, Antel SB, Andermann F, Arnold DL. Mesial temporal damage in temporal lobe epilepsy: a volumetric MRI study of the hippocampus, amygdala and parahippocampal region. Brain 2003;126:462–469.
17. Arsigny V, Fillard P, Pennec X, Ayache N. Log-Euclidean metrics for fast and simple calculus on diffusion tensors. Magn Reson Med 2006;56:411–421.
18. Wakana S, Jiang H, Nagae-Poetscher LM, van Zijl PC, Mori S. Fiber tract-based atlas of human white matter anatomy. Radiology 2004;230:77–87.
19. Catani M, Thiebaut de Schotten M. A diffusion tensor imaging tractography atlas for virtual in vivo dissections. Cortex 2008;44:1105–1132.
20. Worsley KJ, Andermann M, Koulis T, MacDonald D, Evans AC. Detecting changes in nonisotropic images. Hum Brain Mapp 1999;8:98–101.
21. Kuzniecky R, Bilir E, Gilliam F, Faught E, Martin R, Hugg J. Quantitative MRI in temporal lobe epilepsy: evidence for fornix atrophy. Neurology 1999;53:496–501.
22. Schramm J. Temporal lobe epilepsy surgery and the quest for optimal extent of resection: a review. Epilepsia 2008; 49:1296–1307.
23. Yu JT, Tan L. Diffusion-weighted magnetic resonance imaging demonstrates parenchymal pathophysiological changes in epilepsy. Brain Res Rev 2008;59:34–41.
24. Scott RC, King MD, Gadian DG, Neville BG, Connelly A. Prolonged febrile seizures are associated with hippocampal vasogenic edema and developmental changes. Epilepsia 2006;47:1493–1498.
25. Kendal C, Everall I, Polkey C, Al-Sarraj S. Glial cell changes in the white matter in temporal lobe epilepsy. Epilepsy Res 1999;36:43–51.
26. Thom M, Sisodiya S, Harkness W, Scaravilli F. Microdysgenesis in temporal lobe epilepsy: a quantitative and immunohistochemical study of white matter neurones. Brain 2001;124:2299–2309.
27. Salmenpera TM, Simister RJ, Bartlett P, et al. High-resolution diffusion tensor imaging of the hippocampus in temporal lobe epilepsy. Epilepsy Res 2006;71:102–106.
28. Hufnagel A, Weber J, Marks S, et al. Brain diffusion after single seizures. Epilepsia 2003;44:54–63.

29. Thivard L, Lehericy S, Krainik A, et al. Diffusion tensor imaging in medial temporal lobe epilepsy with hippocampal sclerosis. Neuroimage 2005;28:682–690.
30. Focke NK, Yogarajah M, Bonelli SB, Bartlett PA, Symms MR, Duncan JS. Voxel-based diffusion tensor imaging in patients with mesial temporal lobe epilepsy and hippocampal sclerosis. Neuroimage 2008;40:728–737.
31. Ahmadi ME, Hagler DJ Jr, McDonald CR, et al. Side matters: diffusion tensor imaging tractography in left and right temporal lobe epilepsy. AJNR Am J Neuroradiol 2009;30:1740–1747.
32. Concha L, Beaulieu C, Gross DW. Bilateral limbic diffusion abnormalities in unilateral temporal lobe epilepsy. Ann Neurol 2005;57:188–196.
33. Concha L, Livy DJ, Beaulieu C, Wheatley BM, Gross DW. In vivo diffusion tensor imaging and histopathology of the fimbria-fornix in temporal lobe epilepsy. J Neurosci 2010;30:996–1002.

Thank you, Dr. John F. Kurtzke!

The *Neurology*® online archive has recently been updated to include the following issues:

- June 1968; 18 (6 Part 2):1–10
- May 1970; 20 (5 Part 2):1–59
- February 1988; 38 (2):309–316

The Editorial Office acknowledges Dr. John F. Kurtzke for his assistance in filling these gaps.

Practicing Neurologists: Take Advantage of These CMS Incentive Programs

Medicare Electronic Health Records (EHR) Incentive Program
The Medicare EHR Incentive Program provides incentive payments to eligible professionals, eligible hospitals, and critical access hospitals as they adopt, implement, upgrade or demonstrate meaningful use of certified EHR technology. Through successful reporting over a five-year period, neurologists are eligible for up to $44,000 through the Medicare incentive program. To earn the maximum incentive amount, eligible professionals must begin demonstrating meaningful use by October 3, 2012. Learn more at *www.aan.com/go/practice/pay/ehr.*

Medicare Electronic Prescribing (eRx) Incentive Program
The Medicare eRx Incentive Program provides eligible professionals who are successful electronic prescribers a 1% incentive for meeting reporting requirements during the 2012 calendar year. To be eligible, physicians must have adopted a "qualified" eRx system in order to be able to report the eRx measure. This program has also begun assessing payment adjustments for eligible professionals who have not yet begun participation in the program. Learn more at *www.aan.com/go/practice/pay/eRx.*

Physician Quality Reporting System (PQRS)
The Physician Quality Reporting System provides an incentive payment for eligible professionals who satisfactorily report data on quality measures for covered professional services furnished to Medicare beneficiaries. Eligible professionals who report successfully in the 2012 PQRS Incentive Program are eligible to receive a 0.5% bonus payment on their total estimated Medicare Part B Physician Fee Schedule allowed charges for covered professional services. Learn more at *www.aan.com/go/practice/pay/pqrs.*